Int. J. Multiphase Flow Vol. 19, No. 5, pp. 721–735, 1993
Printed in Great Britain.

0301-9322/93 $6.00 + 0.00

DROP PROPERTIES AFTER SECONDARY BREAKUP

L.-P. HSIANG and G. M. FAETH†
Department of Aerospace Engineering, The University of Michigan, Ann Arbor, MI 48109-2140, U.S.A.

(Received 15 December 1992; in revised form 21 June 1993)

Abstract—Drop properties during and after secondary breakup in the bag, multimode and shear breakup regimes were observed for shock-wave-initiated disturbances in air at normal temperature and pressure. Test liquids included water, *n*-heptane, ethyl alcohol and glycerol mixtures to yield Weber numbers of 15–600, Ohnesorge numbers of 0.0025–0.039, liquid/gas density ratios of 579–985 and Reynolds numbers of 1060–15080. Measurements included pulsed shadowgraphy and double-pulsed holography to find drop sizes and velocities after breakup. Drop size distributions after breakup satisfied Simmons' universal root normal distribution in all three breakup regimes, after removing the core (or drop-forming) drop from the drop population for shear breakup. The size and velocity of the core drop after shear breakup was correlated separately based on the observation that the end of drop stripping corresponded to a constant Eötvös number. The relative velocities of the drop liquid were significantly reduced during secondary breakup, due both to the large drag coefficients caused by drop deformation and the reduced relaxation times of smaller drops. These effects were correlated successfully based on a simplified phenomenological theory.

Key Words: drop breakup, drop dynamics, drop deformation, pulsed holography

1. INTRODUCTION

Numerous studies of secondary drop breakup have been reported due to applications for liquid atomization, industrial and agricultural sprays, dispersed multiphase flows and rainfall, among others. In particular, recent studies suggest that secondary breakup is a rate-controlling process in the near-injector region of pressure-atomized sprays through its affect on drop sizes (Ruff *et al.* 1992). Furthermore, primary breakup at the surface of both nonturbulent and turbulent liquids yields drops that intrinsically are unstable to secondary breakup (Wu & Faeth 1992; Wu *et al.* 1991, 1992). Prompted by these observations, the objective of the present investigation was to extend recent work on secondary breakup caused by well-defined step changes of relative velocities (shock-wave disturbances) in this laboratory (Hsiang & Faeth 1992).

The following discussion of past research on secondary breakup is brief, see Hsiang & Faeth (1992), Wierzba & Takayama (1987), Giffen & Muraszew (1953), Hinze (1955), Krzeczkowski (1980), and references cited therein, for more complete reviews. High-speed photography has been used to identify secondary breakup regimes for shock-wave disturbances (Hinze 1955; Hanson *et al.* 1963; Reinecke & McKay 1969; Reinecke & Waldman 1970; Ranger & Nicholls 1969; Gel'fand *et al.* 1974; Krzeczkowski 1980; Wierzba & Takayama 1988). Bag breakup is observed at the onset of secondary breakup. This process involves deflection of the center of the drop into a thin bag, followed by breakup of both the bag and the liquid ring at its base into drops. Shear breakup is observed at higher relative velocities. This process involves stripping of drops from the periphery of the original drop. Finally, the transition between the bag and shear breakup regimes involves a complex combination of behavior at these two limits. This regime will be termed multimode breakup, following Hsiang & Faeth (1992), but it also has been called parachute breakup, chaotic breakup, bag-jet breakup and transition breakup (Krzeczkowski 1980; Wierzba & Takayama 1988). Measurements of transitions between breakup regimes have been limited to liquid/gas density ratios, $\rho_L/\rho_G > 500$ and Reynolds numbers, $\mathrm{Re} = \rho_G d_0 u_0/\mu_G > 500$, where d_0 and u_0 denote the original drop diameter and relative velocity and μ_G is the gas viscosity (Hinze 1955; Krzeczkowski 1980; Hsiang & Faeth 1992). Hinze (1955) shows that breakup regime transitions largely are functions of the ratio of drag/surface tension forces, represented by the Weber number,

†To whom all correspondence should be addressed.

$We = \rho_G d_0 u_0^2/\sigma$, and the ratio of liquid viscous/surface tension forces, represented by the Ohnesorge number $Oh = \mu_L/(\rho_L d_0 \sigma)^{1/2}$, where σ = surface tension and μ_L = liquid viscosity. Hinze (1955) found that the progressively larger We were required for the onset of breakup as Oh increases because viscous forces inhibit drop deformation which is the first step in the breakup process. This behavior has been confirmed by later investigations (Krzeczkowski 1980; Hsiang & Faeth 1992).

The time required for breakup is another aspect of secondary breakup that has received significant attention for shock-wave disturbances at $\rho_L/\rho_G > 500$. For low Oh, it has been found that breakup times normalized by the characteristic breakup time of Ranger & Nicholls (1969), which will be defined later, are remarkably independent of the breakup regime and We (Liang *et al.* 1988). As might be expected from the effect of Oh on breakup regimes, however, recent work shows that normalized breakup times tend to increase with increasing Oh (Hsiang & Faeth 1992). Processes of drop deformation and the variation of the drop drag coefficient with time also appear to scale systematically in terms of the characteristic breakup time (Hsiang & Faeth 1992).

In comparison to other breakup properties, available information about the outcome of secondary breakup is rather limited. Nevertheless, measurements of drop size distributions for shock-wave disturbances at $\rho_L/\rho_G > 500$ have been reported by Gel'fand *et al.* (1974) and Hsiang & Faeth (1992). Gel'fand *et al.* (1974) observed a bimodal drop size distribution for bag breakup, and suggested that the small drops largely resulted from breakup of the bag and the large drops from breakup of the liquid ring at the base of the bag. However, the later measurements of Hsiang & Faeth (1992) did not confirm this finding. Instead, drop size distributions satisfied the universal root normal distribution with the ratio of the mass median diameter to the Sauter mean diameter, MMD/SMD = 1.2, proposed by Simmons (1977). This distribution also has been effective for drops within dense sprays and after primary breakup (Ruff *et al.* 1992; Wu & Faeth 1992; Wu *et al.* 1991, 1992). An exception to this behavior was shear breakup, where the universal root normal distribution was somewhat distorted at large drop sizes. The universal root normal distribution only involves two parameters; therefore, after fixing MMD/SMD, drop sizes are fully specified by the SMD alone. It was found that the SMD for all breakup regimes could be correlated successfully based on a phenomenological analysis of shear breakup (Hsiang & Faeth 1992). These results, however, raised questions about the mechanism causing secondary breakup to end. In particular, at large values of We, large drops in the size distribution after secondary breakup did not undergo subsequent breakup, even though they were unstable to secondary breakup based on existing breakup criteria—barring unusually large reductions of their relative velocities during the secondary breakup process. Unfortunately, information about drop velocities after secondary breakup was not available, so that the mechanism causing breakup to end was not resolved. In addition, information about drop size and velocity correlations after secondary breakup clearly is needed for rational estimates of secondary breakup properties in dispersed flows.

The objective of the present investigation was to extend the work of Hsiang & Faeth (1992) in order to resolve the problems of drop size distributions after shear breakup, the mechanism causing breakup to end, and drop size/velocity correlations after secondary breakup. Experimental methods involved shock-wave-induced disturbances in air with shadowgraph motion picture photography and pulsed holography used to observe the breakup process. The study was limited to conditions representative of bag, multimode and shear breakup near atmospheric pressure: $\rho_L/\rho_G > 500$, $Oh < 0.039$ and $Re > 100$. Water, *n*-heptane, ethyl alcohol and various glycerol mixtures were used as test liquids in order to resolve effects of liquid properties. Phenomenological descriptions of various aspects of secondary breakup were used to help interpret and correlate the measurements.

The paper begins with a discussion of experimental methods. Results are then considered, treating drop size distributions, the properties of the core (or drop-forming) drop when shear breakup ends, and drop velocities after secondary breakup in all three breakup regimes, in turn.

2. EXPERIMENTAL METHODS

2.1. Apparatus

The test apparatus was the same as that of Hsiang & Faeth (1992) and only will be described briefly. A shock tube with the driven section open to the atmosphere, similar to Ranger & Nicholls

(1969), was used for the experiments. The driven section had a rectangular cross section (38 mm wide × 64 mm high) and a length of 6.7 m with the test location 4.0 m from the downstream end. This provided test times of 17–21 ms in the uniform flow region behind the incident shock wave.

The test location had quartz windows (25 mm high × 305 mm long, mounted flush with the interior of the side walls) to allow observations of drop breakup. A drop generator using a vibrating capillary tube, similar to Dabora (1967), was used to generate a stream of drops. This drop stream passed through 6 mm dia holes in the top and bottom of the driven section, crossing the central plane of the driven section at the test location. An electrostatic drop selection system, similar to Sangiovanni & Kestin (1977), was used to deflect a fraction of the drops out of the stream. This yielded a drop spacing of roughly 7 mm so that drops always were present in the region observed while interactions between drops during secondary breakup were eliminated.

2.2. Instrumentation

Breakup properties were recorded using pulsed shadowgraph motion pictures and double-pulsed holography. Pulsed shadowgraph motion pictures were used to observe the overall dynamics of breakup, e.g. drop velocities prior to the onset of breakup and the properties of the core drop, using an arrangement similar to Hsiang & Faeth (1992). This involved a copper vapor laser as the light source with a 35 mm drum camera used to record shadowgraph images at unity magnification. A function generator was used to pulse the laser when the shock wave neared the drop stream location, with pulse frequencies of 6–8 kHz for 20 pulses. Each laser pulse duration was 30 ns which was sufficient to stop the motion of the drop on the rotating film drum. The drum camera recorded the images with an open shutter within a darkened room. The time between shadowgraph pictures was monitored by recording signal generator output using a digital oscilloscope. The film records were analyzed using a Gould FD 5000 image display. The procedure was to obtain three motion picture shadowgraphs for a particular test condition and group the data to obtain statistically-significant results as ensemble averages. Experimental uncertainties (95% confidence) of the measurements reported here are as follows: initial drop diameter and diameter of the core drop at the end of shear breakup, $< 10\%$; and velocity and position of the core drop at the end of shear breakup, $< 15\%$.

Double-pulsed holography was used to measure drop size and velocity correlations after secondary breakup. The holocamera and reconstruction systems were similar to those of Hsiang & Faeth (1992). An off-axis arrangement was used with optics providing a 2–3:1 magnification of the hologram image, and laser pulse time of 20 ns which was sufficient to stop the motion of the drops on film. This was coupled with reconstruction optics that allowed drop diameters as small as 25 μm to be measured with 5% accuracy and drops as small as 10–15 μm to be observed. Reconstruction of the double-pulse holograms yielded two images of the spray with separation times as short as 1 μs. The second pulse was somewhat weaker than the first pulse which allowed directional ambiguity to be resolved because the stronger pulse yielded a sharper reconstructed image. The properties of the reconstructed images were observed using the Gould FD 5000 Image Display with a field view of 1.7 × 2.0 mm. Various locations in the hologram reconstruction were observed by traversing the hologram in two directions and the videocamera of the image display in the third direction.

Drops were sized in the same manner as by Hsiang & Faeth (1992). The diameters of mildly irregular objects were found by measuring their maximum and minimum diameters, d_{max} and d_{min}, through the centroid of the image. Then assuming that the drop had an ellipsoidal shape, the drop diameter was taken to be the diameter, d, of a sphere having the same volume, $d^3 = d_{min}^2\, d_{max}$, as the ellipsoid. More irregular images were sized by finding the cross-sectional area and perimeter of the image and proceeding as before for an ellipsoid having the same properties. The velocity of each drop was found by measuring the distance between the centroid of its two images and dividing by the known time between laser pulses. Results at each condition were summed over at least three realizations, considering 150–300 liquid elements, in order to provide drop size and velocity correlations. Experimental uncertainties caused by the definition of drop diameters are difficult to quantify, however, they are felt to be small in comparison to the accuracy of the size and distance measurements, sampling limitations and effects of grouping of data when velocities were found for a particular drop size. Estimated experimental uncertainties (95% confidence) based on the latter effects are $< 10\%$ for drop diameters and $< 15\%$ for drop velocities.

2.3. Test Conditions

The test conditions are summarized in table 1. Test drops of water, *n*-heptane, ethyl alcohol and various glycerol mixtures were used to provide a wide range of liquid properties. The liquid properties listed in table 1 were obtained from Lange (1952), except for the surface tension of the glycerol mixtures which was measured in the same manner as Wu *et al.* (1991). Initial drop diameters were 1000 μm with the following ranges of other variables: $\rho_L/\rho_G = 580$ to 985, Oh = 0.0025 to 0.039, We = 15 to 600 and Re = 1060 to 15080. The We range includes the bag, multimode and shear breakup regimes, which begin at We = 13, 35 and 80 respectively, based on the measurements of Hsiang & Faeth (1992). The Re range of the present experiments is higher than conditions where gas viscosity plays a significant role on drop drag properties, e.g. the drag coefficient, C_D, for spheres only varies in the range 0.4–0.5 (White 1974). Shock Mach numbers were relatively low, 1.08–1.31, so that physical properties within the uniform flow region were not significantly different from room air.

3. RESULTS

3.1. Drop Size Distributions

It was necessary to address drop size distributions after secondary breakup first because this affects the information needed to characterize secondary breakup properties and drop size and velocity correlations. The main issue to be examined was the distortion of the universal root normal size distribution at large drop sizes after shear breakup, observed by Hsiang & Faeth (1992).

The difficulty with the size distribution function for shear breakup appeared to be due to the presence of the core (or drop-forming) drop, which is the remaining portion of the original drop after the stripping of smaller drops has ended. In particular, the core drop is one of the largest drops in the distribution which corresponded to the region where the measured drop dize distribution departed from the universal root normal distribution. Thus, it seemed plausible that the size distribution would approximate the root normal distribution if the core drop was removed from the drop population.

The resulting drop size distributions after shear breakup, with the core drop removed from the drop population, are illustrated in figure 1. These measurements were obtained directly from the data of Hsiang & Faeth (1992). The results are plotted in terms of the root normal distribution function, with the function itself illustrated for values of MMD/SMD = 1.0, 1.20 and 1.50. The measurements are somewhat scattered at large drop sizes because the number of large drops is limited from the breakup of single drops. In view of this effect, the measured drop size distributions are represented reasonably well by the root normal distribution function with MMD/SMD = 1.2. This behavior is similar to drop size distributions after primary breakup and within dense sprays, as well as for secondary breakup in the bag and multimode breakup regimes (Hsiang & Faeth 1992). Thus, the complication of distortion of the drop size distribution for shear breakup can be handled by treating the core drop separately from the population of the drops stripped from the original drop.

As noted earlier, the universal root normal drop size distribution is specified completely if the SMD is known because the only other parameter in the distribution is fixed, e.g. MMD/SMD = 1.2.

Table 1. Summary of test conditions[a]

Drop liquid	ρ_L (kg/m^3)	$\mu_L \times 10^4$ (kg/ms)	$\sigma \times 10^3$ (N/m)	Oh	We	Re
Water	997	8.94	70.8	0.0038	15–600	1990–15080
n-Heptane	683	3.94	20.0	0.0025	15–600	1060–7200
Ethyl alcohol	800	16.0	24.0	0.011	15–600	1150–7880
Glycerol (42%)[b]	1105	35.0	65.4	0.012	15–375	1910–10790
Glycerol (63%)[b]	1162	108.0	64.8	0.039	15–37	1880–10640

[a]Breakup in air initially at 98.8 kPa and 297 ± 2 K in the driven section of the shock tube with shock Mach numbers in the range 1.08–1.31. Properties of air taken at normal temperature and pressure: $\rho_G = 1.18$ kg/m^3, $\mu_G = 18.5 \times 10^{-6}$ kg/ms.
[b]Percentage glycerin by mass.

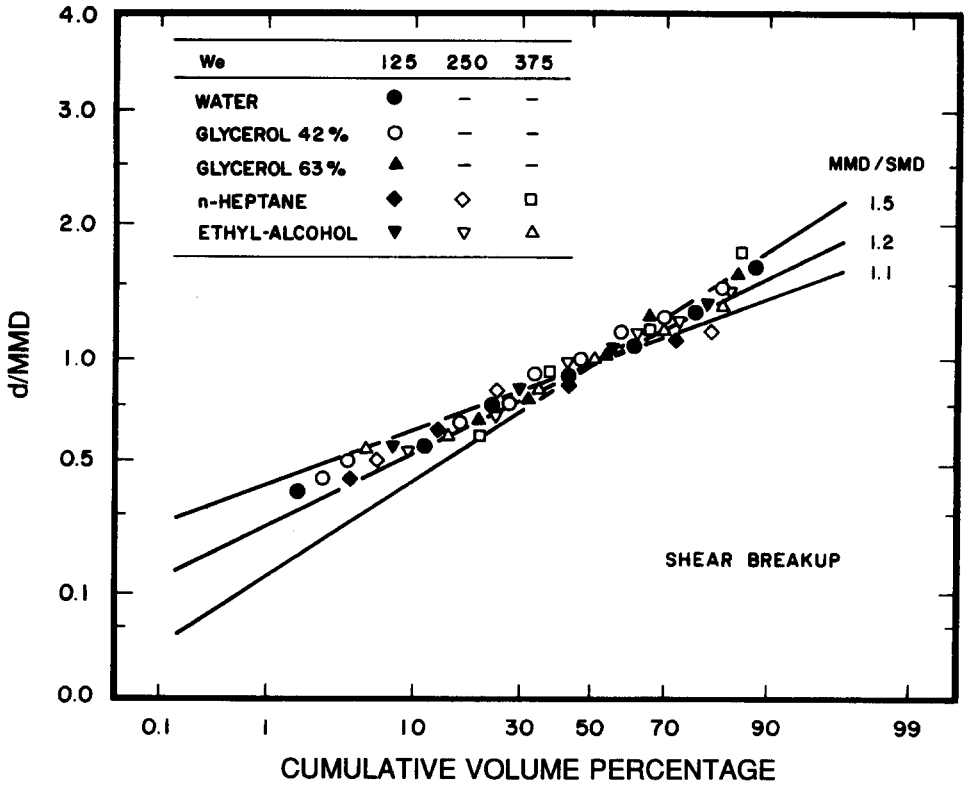

Figure 1. Drop diameter distribution after shear breakup, excluding the core drop.

In principle, the SMD can be found from the correlation given by Hsiang & Faeth (1992) which was obtained using results in the bag, multimode and shear breakup regimes. Fortunately, removing the core drop from the drop population when finding the SMD for shear breakup has a negligible effect on this correlation for available test conditions, in comparison to experimental uncertainties. Thus, use of the correlation of Hsiang & Faeth (1992) for all three breakup regimes is recommended as before, with the properties of the core drop after shear breakup then added to the distribution.

3.2. Core Drop Velocity

The velocity and size of the core drop at the end of breakup must be known, in order to treat it separately from the rest of the drop population after shear breakup. Since drops stripped from the core drop were not observed to undergo subsequent breakup, the end of shear breakup coincides with the end of drop stripping from the core drop. In the following, the velocity of the core drop at the end of breakup will be considered first. Then given information about core drop velocities, subsequent stability considerations yield its size.

In order to assist data correlation, a simplified analysis was used to estimate core drop velocities at the end of breakup. The major assumptions of the analysis are as follows: virtual mass, Bassett history and gravitational forces were ignored; gas velocities were assumed to be constant; mass stripping from the core drop was ignored; and a constant average drag coefficient was used over the period of breakup. For present conditions, virtual mass and Bassett history forces are small due to the large liquid/gas density ratio of the flow (Faeth 1987). Similarly, gravitational forces are not a factor. e.g. drop motion was nearly horizontal and drag forces were much larger than gravitational forces. Uniform gas properties, were a condition of the present experiments. However, the constant core drop mass assumption, taken to be the original drop mass, is questionable. For example, core drop diameters only were 12–30% of the original drop diameter for present test conditions so that the bulk of the original drop mass was lost during stripping. Nevertheless, selecting some other average drop size over the period of breakup only introduces factors on the

order of unity so that the original size of the drop was chosen for convenience. Similarly, drop drag coefficients, C_D, based on the original drop size vary considerably over the drop breakup period. For example, in the deformation period prior to breakup, C_D varies from values 0.4–0.5 at the start of breakup to 4.8–6.4 when the maximum deformation conditions is reached, over the present test range (Hsiang & Faeth 1992). Subsequently, values of C_D based on d_0 become even larger due to the increased responsiveness of the core drop as it becomes smaller. Nevertheless, the scaling of C_D was such that an effective average value could be found to correlate core drop velocities in spite of the crudeness of the approximations of the analysis.

Based on the previous assumptions, conservation of momentum yields the following equation for the motion of the core drop:

$$du/dt = -3\bar{C}_D\rho_G u^2/(4\rho_L d_0), \quad [1]$$

where u is the relative velocity at time t after the arrival of the shock wave disturbance and $\bar{C}_D$ is an approximate average drag coefficient over the time of breakup. Integrating [1] yields the relative velocity of the core drop during the breakup period, as follows:

$$u = u_0/[1 + (3\bar{C}_D t/4t^*)(\rho_G/\rho_L)^{1/2}], \quad [2]$$

where t^* is the characteristic breakup time of Ranger & Nicholls (1969), e.g. $t^* = d_0(\rho_L/\rho_G)^{1/2}/u_0$. Then substituting the breakup time, t_b, into [2], and rearranging, yields the following expression for the absolute velocity of the core drop at the end of breakup, $u_b' = u_0 - u_b$, where u_b is the relative velocity at the end of breakup, as follows:

$$(u_b'/u_0)(\rho_L/\rho_G)^{1/2}(1 + 3C) = 3\bar{C}_D(t_b/t^*)/4, \quad [3]$$

where

$$C = (3\bar{C}_D t_b/4t^*)(\rho_G/\rho_L)^{1/2}. \quad [4]$$

Earlier work has shown that $t_b/t^* = 5$ for $10 < We < 10^6$ and $Oh < 0.1$ (Liang *et al.* 1988; Hsiang & Faeth 1992). Thus, the right-hand side of [3] should be a constant if a constant average value of C_D for the shear breakup process can be found. A reasonable correlation of the present measurements of u_b'/u_0 was obtained by taking $\bar{C}_D = 5$, which is comparable to values observed near the maximum deformation condition (Hsiang & Faeth 1992). This yields $3\bar{C}_D(t_b/t^*)/4 = 19$ on the right-hand side of [3].

The measurements of core drop velocities at the end of breakup, normalized as suggested by [3], are plotted as a function of We in figure 2. Measurements are shown for all the drop liquids over the test range of the shear breakup regime, $100 < We < 600$, along with the fitted prediction of [3]. The correlation for u_b'/u_0 is relatively independent of We over this range as anticipated from [3]. The measurements also are in fair agreement with [3], based on the estimates of t_b/t^* and $\bar{C}_D$ discussed earlier.

The velocity measurements indicated that the relative velocity of the core drop at the end of breakup only was 30–40% lower than the initial relative velocity. This implied that the local We of the core drop when breakup ended generally were greater than the critical Weber number (We_{cr}) for the onset of drop breakup due to shock-wave disturbances ($We = 13$). Thus, the criterion for the end of drop stripping from the core drop differs from the criterion for the onset of breakup. A discussion of this behavior, which leads to an estimation of the core drop diameter, will be considered next.

3.3. Core Drop Size

The dynamic state of a drop at the start of secondary breakup, where the drop is round and the drop liquid is motionless, clearly differs from the state of the core drop when shear breakup ends, where the drop is deformed and liquid motion associated with drop stripping is present. Thus, it is not surprising that local We of the core drop at the end of shear breakup, We_{cr}, are different from (and generally exceed) the We_{cr} associated with the onset of secondary breakup. Instead, conditions defining the end of drop stripping for shear breakup appear to be related more closely to the onset of breakup for more gradual drop motions, such as the breakup of freely-falling drops.

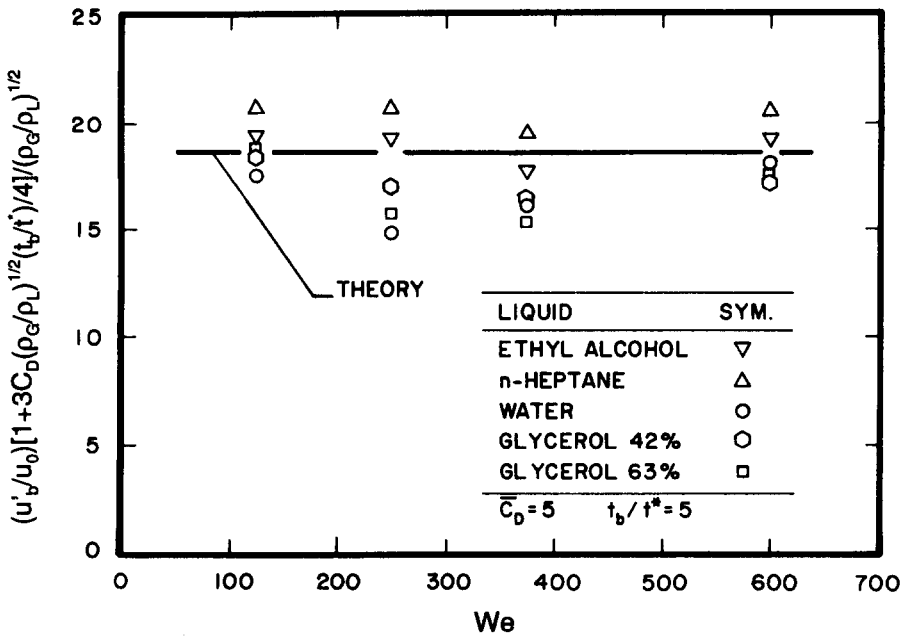

Figure 2. Velocities of the core drop at the end of shear breakup.

This correspondence is exploited in the following to find a criterion for the end of core drop stripping and a method for estimating the size of the core drop at this condition.

The deformation and size of freely-falling drops generally are correlated in terms of the Eötvös number, Eo. The appropriate expression when the drop acceleration, a, is due to gas motion relative to the drop is as follows (Clift *et al.* 1978):

$$\mathrm{Eo} = a|\rho_L - \rho_G|d^2/\sigma \approx a\rho_L d^2/\sigma, \qquad [5]$$

where the latter approximation follows because $\rho_L/\rho_G \gg 1$ for present test conditions. It is anticipated that drop stripping ends when a critical value of Eötvös number, Eo_{cr}, is reached, based on the behavior of freely-falling drops. The acceleration of the core drop can be found by differentiating [2] with respect to time, because this expression provided reasonably good estimates of core drop velocities at the end of breakup (cf. figure 2). This yields

$$a = (3\bar{C}_D u_0/4t^*)(\rho_G/\rho_L)^{1/2}(1 + Ct/t_b)^2. \qquad [6]$$

Then evaluating [6] at $t = t_b$, substituting this value of the acceleration into [5], and noting that $d = d_b$ at t_b, yields the following expression for the Eo_{cr} at the end of shear breakup:

$$\mathrm{Eo}_{cr} = (3\bar{C}_D \mathrm{We}/4)(d_b/d_0)^2/(1 + C)^2. \qquad [7]$$

The values of Eo_{cr} were found for all shear breakup conditions, using $t_b/t^* = 5$ and $\bar{C}_D = 5$ as before. The resulting values of Eo_{cr} for ethyl alcohol, *n*–heptane and water drops are plotted as a function of We in figure 3. Results for the glycerol mixtures are not included in the plot because an effect of Oh_{cr} was observed, tending to increase Eo_{cr}, that is currently being studied for a wider variation of liquid viscosities. Similar to u_b/u_0 in figure 2, the Eo_{cr} of the core drop at the end of shear breakup is relatively independent of We and liquid type over the range of the measurements, yielding a mean value, $\mathrm{Eo}_{cr} = 16$. This behavior also is similar to the breakup requirements of freely-falling drops, as discussed later.

Given Eo_{cr} and the initial conditions of breakup, [7] can be solved to find the diameter of the core drop at the end of shear breakup, d_b. It also is of interest to examine the Weber number of the core drop at this condition, We_{cr}. This can be done by finding u_b and d_b from [3] and [6] and

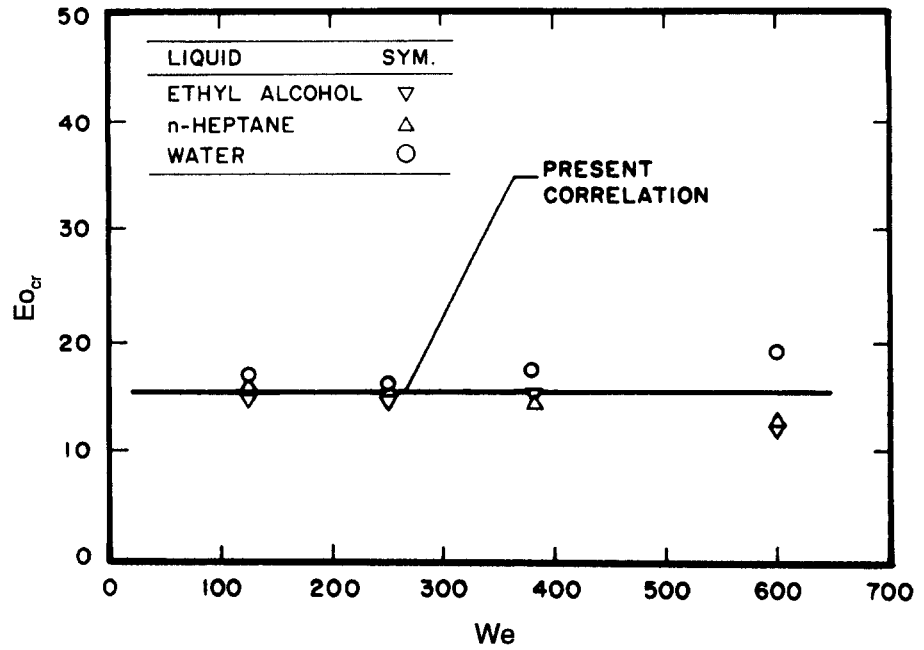

Figure 3. Eo_{cr} of the core drop at the end of shear breakup.

substituting into the normal definition of We, noting that the relative velocity of the core drop is $u_0 - u_b'$, to yield:

$$We_{cr} = (4Eo_{cr}We/3\bar{C}_D)^{1/2}/(1 + C). \quad [8]$$

Adopting $Eo_{cr} = 16$ and $\bar{C}_D = 5$ as discussed earlier, the coefficient in [8], $(4Eo_{cr}/3\bar{C}_D)^{1/2} = 2.3$.

The present measurements of We_{cr} for shear breakup are plotted as suggested by [8] in figure 4. Similar to figure 3, these results are limited to ethyl alcohol, *n*-heptane and water drops, pending resolution of the large Oh_{cr} effects observed for the glycerol mixtures. The range of the

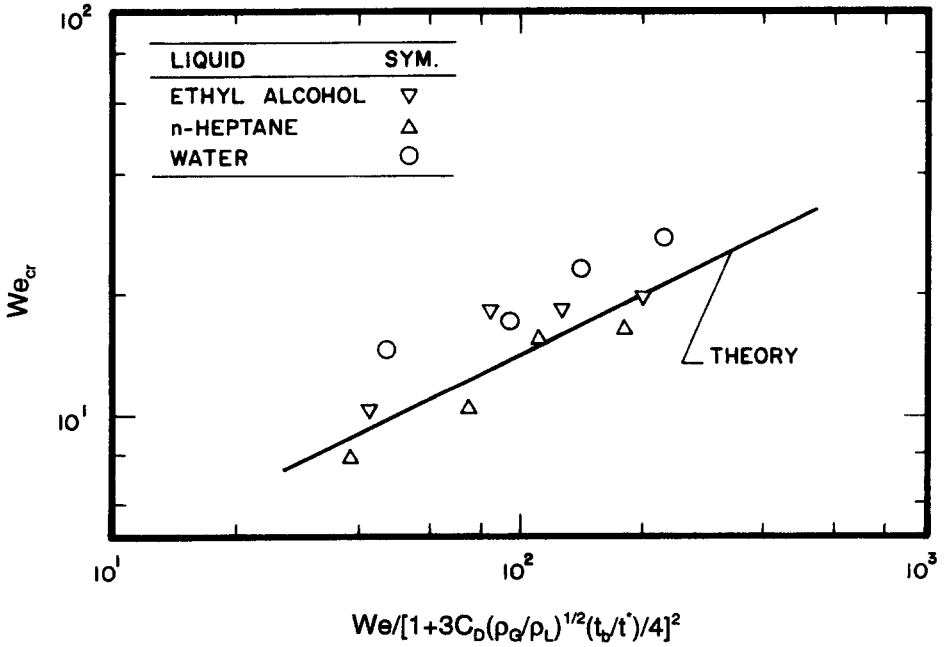

Figure 4. We_{cr} of the core drop at the end of shear breakup.

Table 2. Eo_{cr} for gradual termination and initiation of drop breakup

Drop liquid	d (mm)	ρ_L (kg/m^3)	$\mu_L \times 10^4$ (kg/ms)	$\sigma \times 10^3$ (N/m)	Oh_{cr}	We_{cr}	Eo_{cr}
(a) End of shear breakup							
In air, present study:							
Water	0.15–0.30	997	8.9	71	0.007–0.010	15.1–28.5	17.5
n-Heptane	0.12–0.26	694	4.0	20	0.007–0.010	7.8–16.0	14.9
Ethyl alcohol	0.13–0.29	800	16.0	24	0.021–0.032	10.5–19.0	14.4
(b) Initiation of bag breakup of freely-falling drops							
In air, Merrington & Richardson (1947):							
Water	10.0	1000	9.8	72	0.0012	—	13.5
Carbon tetachloride	3.6	1577	7.8	41	0.0018	—	8.0
In air, Finlay (1957):							
Water	8.0	1000	9.8	72	0.0013	11.0	8.5
Tetrabromomethane	3.5	2950	92.9	36	0.0150	12.0	7.2
In air, Ryan (1976):							
Water	9.1	1000	9.8	72	—	12.2	11.2
Water + surfactant	7.5	1000	—	50	—	12.4	11.1
Water + surfactant	6.9	1000	—	40	—	—	11.6
Water + surfactant	6.1	1000	—	33	—	14.5	12.2
Water + surfactant	5.2	1000	—	25	—	—	10.6
Water + surfactant	4.7	1000	—	20	—	—	10.9
Water + surfactant	4.4	1000	—	17	—	12.0	11.0
In water, Hu & Kintner (1955):							
Tetrabromomethane	5.1	2950	92.9	36	0.0126	7.4	13.8
Dibromoethane	6.7	2150	15.8	32	0.0023	8.2	16.0
Ethyl bromide	9.1	1448	4.9	30	0.0008	7.0	12.3
Nitrobenzene	15.4	1195	17.4	24	0.0026	8.6	19.1
Bromobenzene	11.3	1488	10.7	38	0.0013	7.8	13.5
Tetrachloroethylene	10.4	1614	9.0	44	0.0010	8.2	14.8
Carbon tetrachloride	10.4	1577	7.8	41	0.0009	7.9	15.1

measurements is $100 < We < 1000$. Finally, [8] is illustrated on the plot, using the fitted values of Eo_{cr}, $\bar{C}_D$ and t_b/t^* discussed earlier. The scatter of the data is relatively large because products of the measurements are involved, e.g. $We_{cr} = \rho_G d_b (u_0 - u_b)^2/\sigma$. Nevertheless, [8] provides a reasonable fit of the measurements. The results show that the end of drop stripping from the core drop involves a range of We, generally greater than $We_{cr} = 13$, which is the critical condition for the onset of secondary breakup from shock-wave disturbances. This comes about in the formulation because $We_{cr} \sim We^{1/2}$ in [8] so that We_{cr} reaches large values as We increases in the shear breakup regime. Nevertheless, drop stripping still ends at these high values of We_{cr} because the rate of acceleration of the drop is below critical levels for the gradual variation of drop disturbance levels near the end of the shear breakup process.

It is of interest to compare present values of Eo_{cr} at the end of drop stripping from the core drop during shear breakup with values observed for the breakup of freely-falling drops, which also represents a gradual variation of drop disturbance levels. Thus, table 2 is a summary of Eo_{cr} for the core drop at the end of shear breakup, as well as values of Eo_{cr} measured for freely-falling drops of various liquids in both gases and liquids from Merrington & Richardson (1947), Finlay (1957), Ryan (1976) and Hu & Kintner (1955). The conventional definition of the Eötvös number for freely-falling drops is as follows (Clift *et al.* 1978):

$$Eo_{cr} = g|\rho_L - \rho_G|d^2/\sigma, \qquad [9]$$

where d is the maximum stable drop diameter, g is the acceleration of gravity and ρ_G should be interpreted as the density of the continuous phase (and is liquid for freely-falling drops in liquids). In addition to Eo_{cr}, table 2 provides the values of d, ρ_L, μ_L, σ, Oh_{cr} and We_{cr} for the various breakup processes.

For conditions at the end of shear breakup in table 2, d_b, Oh_{cr} and We_{cr} vary over ranges set by the present test conditions, which is evident from figure 4, even though Eo_{cr} is relatively constant. In contrast, stable freely-falling drop conditions involve single values of d, Oh_{cr} and We_{cr} for given

drop and continuous phases. In this case, We_{cr} and Eo_{cr} are closely related because the freely-falling drops eventually stabilize at their terminal velocity where the maximum value of We is reached. Remarkably, the average values of Eo_{cr} are not very different for the end of shear breakup and for the onset of breakup for freely-falling drops in both gases and liquids, 16 and 12, respectively. Differences of this order certainly are reasonable because one process involves the end of drop stripping from the core drop, while the other represents a limit for the onset of bag breakup (Clift *et al.* 1978).

Loparev (1975) reports We_{cr} for the onset of drop breakup, generally by bag breakup, during gradually accelerating and decelerating gas flows in converging passages. An extensive range of conditions was studied but unfortunately the information provided is not sufficient to find values of Eo_{cr}. Nevertheless, values of We_{cr} for low-Oh_{cr} drops are similar to those in table 2 for freely-falling drops, suggesting similar values of Eo_{cr} as well. An interesting aspect of these measurements is that We_{cr} increases with increasing Oh_{cr} for glycerol mixtures, similar to the behavior observed during the present study for the end of shear breakup. This is not surprising, due to past observations of increasing We at the onset of breakup for shock-wave disturbances as Oh increases (Hinze 1955; Krzeczkowski 1980; Hsiang & Faeth 1992). Pending resolution of this issue, however, the present value of Eo_{cr} should be used with caution to find core drop properties when values of $Oh_{cr} > 0.032$.

The previous considerations suggest that We, Eo and time all are factors in drop breakup events at low Oh. These interactions are highlighted by the local values of We_{cr}, Eo_{cr} and t_{cr}/t^* for the various breakup events summarized in table 3. For abrupt disturbances, like the onset of secondary breakup due to shock-wave disturbances, local values of We_{cr} and Eo_{cr} were estimated at the time of breakup using measured values of drop drag in the deformation period. Thus, these values are lower than criteria normally given for breakup regime transitions due to drop acceleration prior to the onset of breakup. Similar to the normalized breakup time, the normalized time at the onset of breakup for shock-wave disturbances is a constant over a wide range of We, $t_{cr}/t^* = 1.6$. For this process, drops in the deformation period have local values of We and Eo that exceed limits for the onset of breakup, however, breakup does not begin until the drop has had time to deform and achieve a dynamical condition in the liquid that allows drops to separate from the parent drop. The characteristics of We_{cr}, Eo_{cr} and t_{cr}/t^* are somewhat different for gradual disturbances. In the case of bag breakup for a freely-falling drop, Eo, based on the actual drop acceleration, is a maximum at the start of free fall while t_{cr}/t^* is large due to the relatively slow acceleration of the drop. Thus, liquid properties are roughly quasisteady at each relative velocity condition and breakup only occurs when forces on the drop surface due to drag are too large to be stabilized by surface tension, i.e. when the We of the drop reaches a critical value. Finally, the end of drop stripping for shear breakup also involves near-quasisteady liquid behavior with the dynamical state of the drop being stabilized by surface tension once the forces on the surface, represented by the drop acceleration, become lower than a critical value represented by Eo_{cr}. A range of We_{cr} is associated with this condition due to the large variation of the drag coefficient with the degree of deformation of the drop. Thus, various breakup events are associated with required minimum values of We, Eo and time, with one of these parameters generally serving as the controlling parameter for a particular process.

Table 3. Criteria for secondary breakup processes[a]

Process	We_{cr}	Eo_{cr}	t_{cr}/t^*
Abrupt (shock-wave) disturbances			
Start of bag breakup (in gases)	8–23	24–70	1.6
Start of multimode breakup (in gases)	23–53	70–160	1.6
Start of shear breakup (in gases)	$\geqslant 53$	$\geqslant 160$	1.6
Gradual disturbances			
Start of bag breakup (in gases)[b]	11–13	11	Large
Start of bag breakup (in liquids)[b]	7–9	15	Large
End of shear breakup (in gases)	8–29[c]	16	5.5

[a]$Oh < 0.05$, We_{cr} and Eo_{cr} subsequently increase with increasing Oh.
[b]Freely-falling drops in a motionless environment.
[c]Present test range with wider range probable.

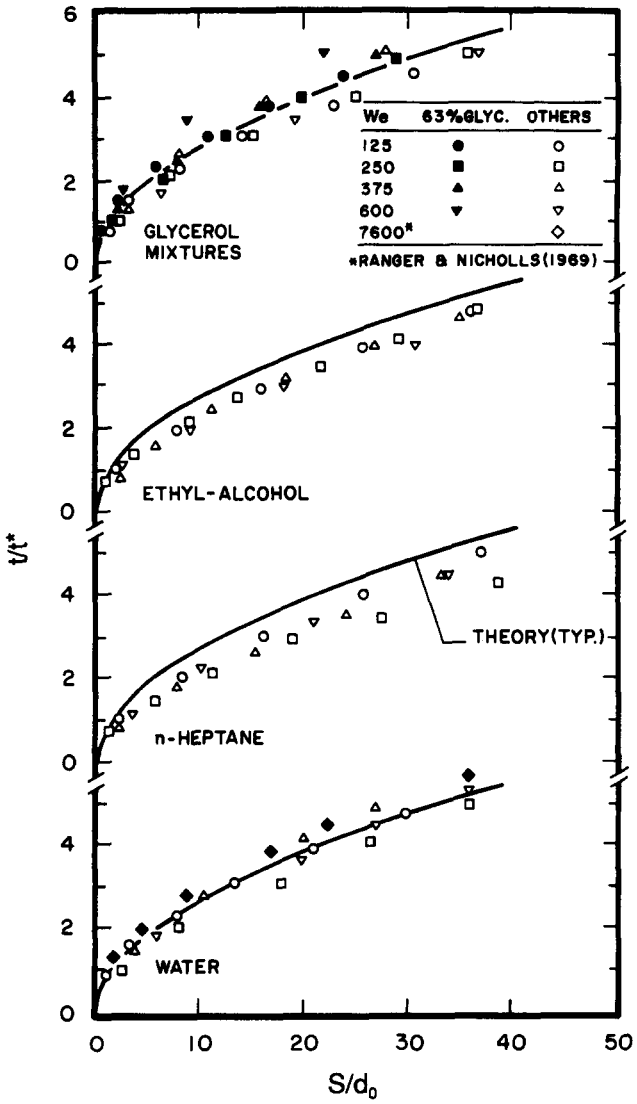

Figure 5. Displacements of core drops during the breakup period.

3.4. *Core Drop Displacement*

The analysis to find core drop velocities after secondary breakup was extended to find the displacement of the core drop as a function of time during secondary breakup. This provides a means of further evaluating the simplified analysis using measurements of core drop displacements, as well as providing a measure of the spatial extent of the shear breakup process.

The displacement of the core drop was found using the same assumptions employed to find the velocity of the core drop at the end of secondary breakup. This involved substituting u from [2] into the expression for the absolute velocity of the core drop, $u' = u_0 - u$, and integrating the resulting expression with respect to time. This yields the following expression for the displacement of the core drop, S, as a function of time after the arrival of the velocity disturbance:

$$S/d_0 = 3\bar{C}_D(t_b/2Ct^*)^2[Ct/t_b - \ln(1 + Ct/t_b)], \qquad [10]$$

where C is found from [4] using $t_b/t^* = 5$ and $\bar{C}_D = 5$, as before. Having made these selections, S/d_0 as a function of t/t^* only varies with the gas/liquid density ratio when C is computed from [4].

Predicted and measured core drop displacements are plotted as a function of time in figure 5. Measured results for the glycerol mixtures are combined on one plot because values of the gas/liquid density ratio are nearly the same for the two mixtures. Results for ethyl alcohol,

n-heptane and water are plotted separately in order to reduce the overlap of the data. The earlier measurements of Ranger & Nicholls (1969) for water also are shown on the plot: these results are in good agreement with the present measurements. In view of the simplifications used to find [10], the comparison between predictions and measurements is reasonably good. The main discrepancies are observed for ethyl alcohol and n-heptane, where the time required to reach a particular displacement is overestimated by roughly 10% for conditions near the end of breakup. Finally, the values of S/d_0 are roughly 40 at the end of breakup, thus, secondary breakup is approximated only crudely as a local event.

3.5. Drop-Size/Velocity Correlation

The last aspect of secondary breakup considered was the drop-size/velocity correlation at the completion of secondary breakup. These results will include all the drops in the bag and multimode breakup regimes. However, the core drop will be excluded in the shear breakup regime because its properties have already been established.

A simplified analysis, similar to the approach used for core drop velocities, was used to assist the correlation of drop velocity data. This involved neglecting virtual mass, Bassett history and gravitational forces and taking gas properties to be constant, as before. It also was assumed that a constant average drag coefficient was appropriate over the period of breakup, but provision was made to vary the average drag coefficient with drop size due to the large range of drop sizes that must be considered. Similarly, drops of various sizes are formed at different times during the breakup period, so that variations of residence times as separated drops in the gas phase were considered as well. Although the resulting approach still is rather crude, it did yield results that were useful for correlating the velocity measurements.

Based on these assumptions, the governing equation of conservation of momentum for a drop having a diameter, d, and relative velocity, u, and an average drag coefficient, $\bar{C}_{Dd}$, is as follows:

$$du/dt = -3\bar{C}_{Dd}\rho_G u^2/(4\rho_L d). \quad [11]$$

integrating [11] from $t = 0$, where $u = u_0$, to $t = t_d$, where $u = u_b$, yields the following expression for the final relative velocity of the drop:

$$u_0/u_b - 1 = (3\bar{C}_D t_b/4t^*)(\bar{C}_{Dd}/\bar{C}_D)(t_d/t_b)(\rho_G/\rho_L)^{1/2}(d_0/d). \quad [12]$$

The functions, $\bar{C}_{Dd}/\bar{C}_D$ and t_d/t_b are unknown but based on [12] it seems reasonable to plot $u_0/u_b - 1$ as a function of $(\rho_G/\rho_L)^{1/2}(d_0/d)$.

The resulting drop-size/velocity correlation based on these considerations is plotted in figure 6. The test results involve all drop liquids over the data range summarized in table 1, including the bag, multimode and shear breakup regimes. Results for the core drops have been shown as dark symbols, for comparison purposes, but they are not included in the following drop-size/velocity correlation. The measured results clearly are independent of the breakup regime and can be correlated reasonably well using the following empirical fit based on [12]:

$$u_0/u_b - 1 = 2.7[(\rho_G/\rho_L)^{1/2}d_0/d]^{2/3}. \quad [13]$$

Thus, the reduction of the power of $[(\rho_G/\rho_L)^{1/2}d_0/d]$ from [12] to [13] is relatively modest in view of potential complications due to $\bar{C}_{Dd}/\bar{C}_D$ and t_d/t_b. Additionally, [13] appears to be rather robust over the three breakup regimes, the range of liquid types and the flow conditions considered during the present experiments. Even the results for core drops are in fair agreement with [13], however, the specific relationships for core drops discussed earlier provide a better estimate of their velocities. Finally, the results indicate that relative velocities are reduced 30–70% over the period of breakup, with the smallest drops experiencing the largest reduction of relative velocity due to their smaller relaxation times.

4. CONCLUSIONS

The outcome of secondary breakup after shock-wave-initiated disturbances was studied, considering drops of water, n-heptane, ethyl alcohol and glycerol in air at normal temperature and

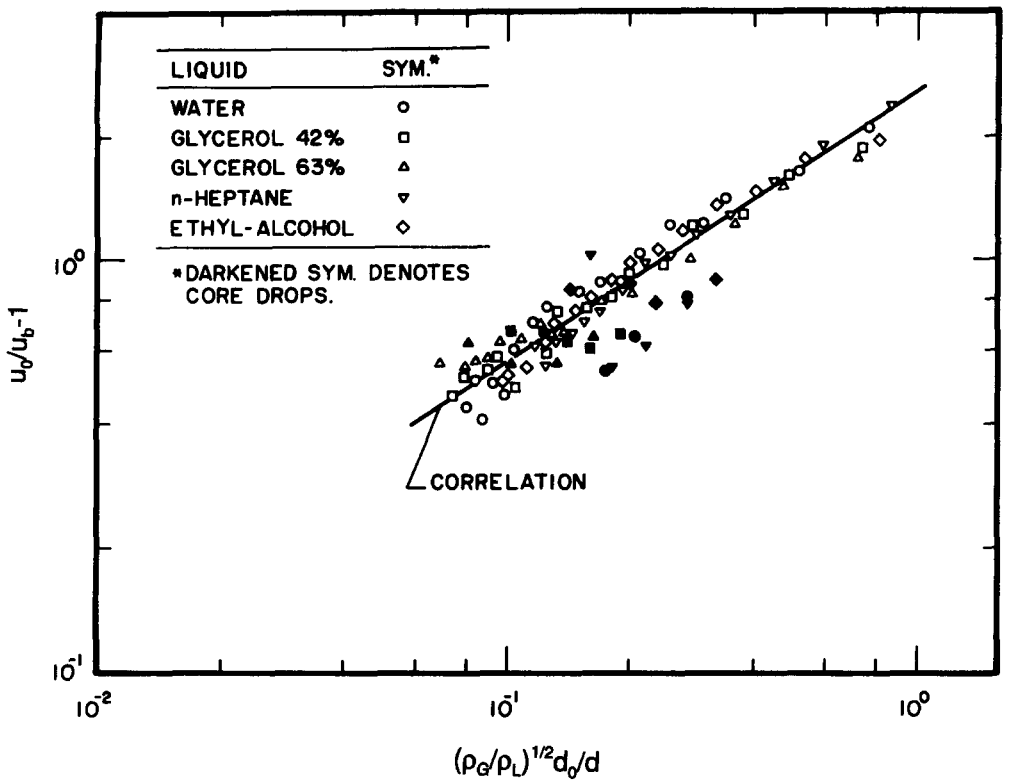

Figure 6. Correlation of drop velocities after secondary breakup as a function of drop size.

pressure (We of 15–600, Oh of 0.0025–0.039, ρ_L/ρ_G of 579–985 and Re of 1060–15080). The major conclusions of the study are as follows:

1. Earlier problems with the drop size distribution after shear breakup (Hsiang & Faeth 1992) were resolved by removing the core drop from the drop population and treating it separately. With this change, drop sizes after breakup in all three breakup regimes satisfy Simmons' universal root normal distribution with MMD/SMD = 1.2. Removal of the core drop from the drop size distribution has a negligible effect on the SMD correlation of Hsiang & Faeth (1992) which can be used as before.
2. The velocity and size of the core drop after shear breakup were correlated and successfully based on simplified considerations of drop motion during breakup, [3], and the observation that the Eo at the end of drop stripping was a constant, [7], i.e. $Eo_{cr} = 16$.
3. The relative velocities of the drop liquid are significantly reduced during secondary breakup (30–70%, depending on drop size) due to the large drag coefficients during the drop deformation stage and the reduced relaxation times of smaller drops. These effects were correlated successfully based on variables from simplified analysis of drop motion (figure 6 and [13]).
4. At low Oh, criteria for various drop breakup processes can be represented by critical values of We, Eo and t/t^*. While certain minimum values are required for all three parameters, reaching a critical local value of one of the parameters tends to control the onset of particular breakup events: t_{cr}/t^* for the onset of breakup after a shock-wave disturbance, We_{cr} for the onset of breakup of a freely-falling drop and Eo_{cr} for the end of drop stripping from the core drop during shear breakup.

The present findings generally were limited to Oh < 0.039, with results concerning core drop properties limited to Oh < 0.011. Increasing Oh tends to impede drop deformation and breakup

processes and should modify secondary breakup behavior considerably from the results observed during the present study. The liquid/gas density ratios of present work also were relatively limited and are most appropriate for sprays at atmospheric pressure. Effects of both Oh and ρ_L/ρ_G clearly merit additional study in order to better understand secondary breakup properties.

Acknowledgements—This research was sponsored by the Air Force Office of Scientific Research, Grant Nos AFOSR-89-0516 and F49620-92-J-0399, under the technical management of J. N. Tishkoff. The authors would like to thank C. W. Kauffman for the loan of the shock tube facility and advice concerning its operation. The U.S. Government is authorized to reproduce and distribute copies for governmental purposes notwithstanding any copyright notation thereon.

REFERENCES

BORISOV, A. A., GEL'FAND, B. E., NATANZON, M. S. & KOSSOV, O. M. 1981 Droplet breakup regimes and criteria for their existence. *Inzh.-Fiz. Zh.* **40,** 64–70.

CLIFT, R., GRACE, J. R. & WEBER, M. E. 1978 *Bubbles, Drops and Particles*, pp. 26 & 339–347. Academic Press, New York.

DABORA, E. K. 1967 Production of monodisperse sprays. *Rev. Scient. Instrum.* **38,** 502–506.

FAETH, G. M. 1987 Mixing, transport and combustion in sprays. *Prog. Energy Combust. Sci.* **13,** 293–345.

FINLAY, B. A. 1957 Ph.D. Thesis, Univ. of Birmingham, W. Midlands, U.K.

GEL'FAND, B. E., GUBIN, S. A. & KOGARKO, S. M. 1974 Various forms of drop fractionation in shock waves and their special characteristics. *Inzh.-Fiz. Zh.* **27,** 119–126.

GIFFEN, E. & MURASZEW, A. 1953 *The Atomization of Liquid Fuels*. Chapman & Hall, London.

HANSON, A. R., DOMICH, E. G. & ADAMS, H. S. 1963 Shock-tube investigation of the breakup of drops by air blasts. *Phys. Fluids* **6,** 1070–1080.

HINZE, J. O. 1955 Fundamentals of the hydrodynamic mechanism of splitting in dispersion processes. *AIChE Jl* **1,** 289–295.

HSIANG, L.-P. & FAETH, G. M. 1992 Near-limit drop deformation and secondary breakup. *Int. J. Multiphase Flow* **18,** 635–652.

HU, S. & KINTNER, R. C. 1955 The fall of single drops through water. *AIChE Jl* **1,** 42–48.

KRZECZKOWSKI, S. A. 1980 Measurement of liquid droplet disintegration mechanisms. *Int. J. Multiphase Flow* **6,** 227–239.

LANGE, N. A. 1952 *Handbook of Chemistry*, 8th edn, pp. 1134 & 1709. Handbook Publishers, Sandusky, OH.

LIANG, P. Y., EASTES, T. W. & GHARAKHARI, A. 1988 Computer simulations of drop deformation and drop breakup. AIAA Paper No. 88-3142.

LOPAREV, V. P. 1975 Experimental investigation of the atomization of drops of liquid under conditions of a gradual rise of the external forces. *Izv. Akad. Nauk SSSR Mekh. Zhidkosti i Gaza* **3,** 174–178.

MERRINGTON, A. C. & RICHARDSON, E. G. 1947 The break-up of liquid jets. *Proc. Phys. Soc. (Lond.)* **59,** 1–13.

RANGER, A. A. & NICHOLLS, J. A. 1969 The aerodynamic shattering of liquid drops. *AIAA Jl* **7,** 285–290.

REINECKE, W. G. & MCKAY, W. L. 1969 Experiments on waterdrop breakup behind Mach 3 to 12 shocks. Report SC-CR-70-6063, Sandia Corp., Albuquerque, NM.

REINECKE, W. G. & WALDMAN, G. D. 1970 A study of drop breakup behind strong shocks with applications to flight. Avco Report AVSD-0110-70-77.

RUFF, G. A., WU, P.-K., BERNAL, L. P. & FAETH, G. M. 1992 Continuous- and dispersed-phase structure of dense nonevaporating pressure-atomized sprays. *J. Propul. Power* **8,** 280–289.

RYAN, R. T. 1976 The behavior of large low-surface-tension water drops falling at terminal velocity in air. *J. Appl. Met.* **15,** 157–165.

SANGIOVANNI, J. & KESTIN, A. S. 1977 A theoretical and experimental investigation of the ignition of fuel droplets. *Combust. Sci. Technol.* **16,** 59–70.

SIMMONS, H. C. 1977 The correlation of drop-size distributions in fuel nozzle sprays. *J. Engng Power* **99,** 309–319.

WHITE, F. M. 1974 *Viscous Fluid Flow.* McGraw-Hill, New York.

WIERZBA, A. & TAKAYAMA, K. 1987 Experimental investigations on liquid droplet breakup in a gas stream. *Rep. Inst. High Speed Mech., Tohoku Univ.* **53,** 1–99.

WIERZBA, A. & TAKAYAMA, K. 1988 Experimental investigation of the aerodynamic breakup of liquid drops. *AIAA Jl* **26,** 1329–1335.

WU, P.-K. & FAETH, G. M. 1992 Aerodynamic effects on primary breakup of turbulent liquids. *Atomiz. Sprays.* In press.

WU, P.-K.. RUFF, G. A. & FAETH, G. M. 1991 Primary breakup in liquid/gas mixing layers. *Atomiz. Sprays* **1,** 421–440.

WU, P.-K., TSENG, L.-K. & FAETH, G. M. 1992 Primary breakup in gas/liquid mixing layers for turbulent liquids. *Atomiz. Sprays* **2,** 295–317.